Fidelity of Binding of the Guanidinium Nucleic Acid (DNG) d(Tg)$_4$-T-azido with Short Strand DNA Oligomers ($A_5G_3A_5$, $GA_4G_3A_4G$, $G_2A_3G_3A_3G_2$, $G_2A_2G_5A_2G_2$). A Kinetic and Thermodynamic Study[†]

Andrei Blaskó, Elvira E. Minyat, Robert O. Dempcy, and Thomas C. Bruice*

Department of Chemistry, University of California, Santa Barbara, California 93106

Received January 13, 1997; Revised Manuscript Received March 27, 1997[⊗]

ABSTRACT: Short strand DNA oligomers ($A_5G_3A_5$, $GA_4G_3A_4G$, $G_2A_3G_3A_3G_2$, and $G_2A_2G_5A_2G_2$) and the guanidinium (g) linked thymidyl nucleoside d(Tg)$_4$-T-azido associate as triplexes. The melting temperatures, T_m, the association and dissociation kinetic and thermodynamic parameters and activation energies for the triplexes were determined by UV thermal analysis. The hypochromic shift and T_m for triplex formation increases with increase in concentration and decreases with the number of mismatches. The melting temperatures are between 35 and 55 °C in the range of ionic strength of 0.06−0.24 and decrease with increase in ionic strength at 100 deg/(ionic strength unit). The melting and cooling curves exhibit hysteresis behavior in the temperature range 5−95 °C at 0.2 deg/min thermal rate. From these curves, the rate constants and the energies of activation for association (k_{on}, E_{on}) and dissociation (k_{off}, E_{off}) processes were obtained. The second-order rate constants, k_{on}, for the triplex formation at 288 K are between 10 and 500 $M^{-1}\ s^{-1}$. Values of k_{on} increase with the decrease in the ionic strength. The first order rate constants for the dissociation, k_{off}, at 288 K are between 10^{-6} and $40 \times 10^{-6}\ s^{-1}$ and increase with increase in ionic strength. The energies of activation for the association and dissociation processes are in the range −22 to −9 kcal/mol and 8 to 29 kcal/mol, respectively. At 6.3×10^{-5} M/base and at the physiological ionic strength (0.15−0.30) and below, the triplex structures formed with d(Tg)$_4$-T-azido and $A_5G_3A_5$ and $GA_4G_3A_4G$ have well-defined T_m values. The melting curves with $G_2A_3G_3A_3G_2$ and $G_2A_2G_5A_2G_2$ are very shallow with small hypochromic shifts denoting negligible binding at physiological ionic strength. Therefore, with the increase in the G content (mismatched base pairs) at a certain concentration (e.g., 6.3×10^{-5} M/base), discrimination (change in fidelity) occurs in the formation and strength of binding of d(Tg)$_4$-T-azido to d(pA$_n$pG$_m$) oligomers. The standard molar enthalpies for triplex formation have in general larger negative values at low ionic strength than at high ionic strength, indicating that at lower μ values the formation of triplexes of d(Tg)$_4$-T-azido with d(pA$_n$pG$_m$) are more favorable. The values of $\Delta H°(288)$ calculated from the activation parameters are between −17 and −49 kcal/mol, and the values of $\Delta G°(288)$ are between −7.5 and −11.8 kcal/mol for $A_5G_3A_5$, $GA_4G_3A_4G$, $G_2A_3G_3A_3G_2$, and $G_2A_2G_5A_2G_2$, respectively. There is a linear relationship in the enthalpy−entropy compensation for the triplex melting thermodynamics.

Replacement of the phosphodiester linkages of DNA and RNA with guanidine (g) linkages provides the polycations deoxyribonucleic and ribonucleic guanidine (DNG and RNG)[1] (Dempcy et al., 1994, 1995a,b, 1996; Browne et al., 1995). The desirability of providing more effective antigene/antisense agents by replacing the phosphodiester linkage of DNA and RNA by linkages which are either neutral or positively charged, and resistant toward nuclease degradation has been discussed (Vasseur et al., 1992; Sanghvi & Cook, 1993; Rouhi, 1996). The triple helical structures (T*A•T) between d(Tg)$_4$-T-azido and d(pA)$_5$ up to d(pA)$_{10}$ were found to have stability constants estimated to exceed that of their DNA counterparts by at least 3 orders of magnitude (Blaskó et al., 1996) (Chart 1). The electrostatic attraction between polycationic d(Tg)$_4$-T-azido and polyanionic d(pA)$_x$ stabilizes the helical hybrid structures as a function of decreasing ionic strength. This relationship was anticipated as d(Tg)$_4$-T-azido provides for an electrostatic binding interaction to DNA in addition to Watson−Crick and Hoogsteen hydrogen bonding interactions. This is of course opposite to the charge repulsion between negative strands of DNA and the increase in stability (i.e., T_m) of dsDNA with increase in ionic strength.

A major feature of the Watson−Crick proposal was the idea that only purine−pyrimidine pairs would be readily accommodated within the structure of the helix, with the specificity of purine−pyrimidine pairing dictated by satisfaction of the hydrogen-bonding potential of the bases (Watson & Crick, 1953). However, other forces, like stacking interactions in conjunction with hydrogen-bonding interactions, can be more important (Guckian et al., 1996) leading to a whole variety of unusual structures, even containing mismatched base pairs.

Our studies have established that d(Tg)$_4$-T-azido does not complex with poly(dG), poly(dC), and poly(dU) but forms very stable [d(Tg)$_4$-T-azido]$_2$•d(pA)$_x$ triplexes. It would

---

[†] We express our appreciation to the Office of Naval Research for support of this study (Grant N00014-96-I-0123).

* To whom all correspondence should be addressed. Fax: (805) 893-2229. E-mail: tcbruice@bioorganic.ucsb.edu.

[⊗] Abstract published in *Advance ACS Abstracts*, June 1, 1997.

[1] Abbreviations: DNG, deoxyribonucleic guanidine; RNG, ribonucleic guanidine; WC, Watson−Crick; Tr, triplex; D, duplex; M, monomer; DSC, differential scanning calorimetry; CD, circular dichroism; UV, ultraviolet; TGGE, temperature-gradient gel electrophoresis.

S0006-2960(97)00064-0 CCC: $14.00

Chart 1

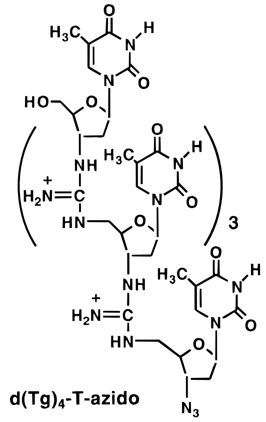

d(Tg)$_4$-T-azido

1. 5'-AAAAAGGGAAAAA-3'
2. 5'-GAAAAGGGAAAAG-3'
3. 5'-GGAAAGGGAAAGG-3'
4. 5'-GGAAGGGGGAAGG-3'

appear that RNG and DNG warrant investigation as sources of antisense/antigene agents (Dempcy et al., 1995a; Blaskó et al., 1996). In this regard, it is important to determine if the fidelity of base recognition between phosphate-linked oligos and guanidinium-linked oligonucleotides is comparable to that observed in double- and triple-stranded complexes involving DNA and RNA oligomers.

Mismatch base pairing, such as G−T, G−G, and G−A interactions, are very important in biological events. The frequency of mutations at a particular site in a genome is in some way a function of the base sequence surrounding that site (Patten et al., 1984). The base sequence at a site can also affect the stability of a mismatch and in some cases the conformation as well (Patten et al., 1984). Misincorporation frequency is increased when the nearest-neighbor nucleotides form more stable base pairs with the corresponding nucleotides in the template and is decreased when they form less stable base pairs (Patten et al., 1984). Both prokaryotes and eukaryotes process mismatched base pairs, pairing errors in which the Watson−Crick bases occur in noncomplementary opposition within the DNA helix (nb; transition mispairs, G−T and A−C; transversion mismatches, G−G, A−A, G−A, C−C, T−T, and C−T) (Modrich, 1987). Such mispairs arise as a consequence of genetic recombination and as a result of DNA biosynthetic errors (Modrich, 1987). Mispairs corresponding to distinct genetic markers can be corrected with different efficiencies, with the implied specificity representing a major argument that mismatches provoke their own repair. The importance of G-rich sequences in biological events reside in the fact that in contrast to the G−T, A−C, A−A, G−G, and T−T point mispairs, the G−A, T−C, and C−C transversion mispairs are generally poor substrates for correction in the bacterial systems (Modrich, 1987). Of interest is that *in vitro* the G−G mismatch is repaired at rates of 40−80% of that of G−T mispair (Su et al., 1988).

The various G content of the DNA oligomers of this work makes possible the study of the G−G, G−T, and G−A interactions. Oligonucleotides containing either two or four runs of guanosines tend to adopt fold-back structures with the guanosines usually adopting alternating *syn* and *anti* orientations [except *Tetrahymena* telomeric repeat, d(TTGGGG)$_4$, where (*anti*)$_3$*syn* and (*syn*)$_3$*anti* patterns are observed along the strands] (Kochoyan & Leroy, 1995). Guanine-rich sequences occur in immunoglobulin switch region (Shimizu & Honjo, 1984), in gene promoters (Evans et al., 1984; Kilpatrick et al., 1986), in chromosomal telomeres (Blackburn & Szostak, 1984), and in a variable number of terminal repeat regions (Sen & Gilbert, 1990).

The behavior of short strand oligomers differs from that of the long strand oligomers and their involvement in genetic disorders is different (Mitchell et al., 1995). The potential role of these structures in biological events can be assessed by sequence-dependent kinetic and thermodynamic data on the stability and conformational flexibility of all secondary structural features (Breslauer, 1986).

In this study, we report the melting temperatures, T_m, as well as the association and dissociation kinetic and thermodynamic parameters for the formation of triplexes with mismatched base pairs of short strand DNA AG oligomers ($A_5G_3A_5$, $GA_4G_3A_4G$, $G_2A_3G_3A_3G_2$, and $G_2A_2G_5A_2G_2$) and the guanidinium (g)-linked thymidyl nucleoside, d(Tg)$_4$-T-azido. We chose these sequences taking into account that d(Tg)$_4$-T-azido forms triplexes with homooligomers having strand lengths >5 [*i.e.,* longer than d(Tg)$_4$-T-azido] in a "domino" fashion (Blaskó et al., 1996). Changing the A residues to G from both ends and in the middle allows similar exposure of d(Tg)$_4$-T-azido strands to the G bases in the complex. The melting temperatures (T_m) serve as a measure of the strength of binding of oligonucleotide strands to form duplexes and triplexes. Heating and cooling plots of mole fractions *vs* temperature in the case of the triplexes of d(Tg)$_4$-T-azido with short strand complementary oligonucleotides provided hysteresis (Blaskó et al., 1996). In general, from the hysteresis shape the individual rates of the association and dissociation of the strands forming duplexes and triplexes and the associated thermodynamic parameters can be determined.

MATERIALS AND METHODS

Materials. The guanidinium-linked thymidyl nucleoside d(Tg)$_4$-T-azido was prepared as reported (Dempcy et al., 1994, 1995a,b). Short strand DNA oligomers $A_5G_3A_5$, $GA_4G_3A_4G$, $G_2A_3G_3A_3G_2$, and $G_2A_2G_5A_2G_2$ were from the University of California at San Francisco, Biomolecular Resource Center.

The concentrations of nucleotide solutions were determined using the extinction coefficients (per mole of nucleotide) calculated according to the nearest-neighbor approximation for the DNA mismatches (Cantor & Tinoco, 1965; Gray et al., 1995): $\epsilon_{260,}$ $M^{-1}cm^{-1}$; $A_5G_3A_5$, 12126; $GA_4G_3A_4G$, 11781; $G_2A_3G_3A_3G_2$, 11588; $G_2A_2G_5A_2G_2$, 11394. For d(Tg)$_4$-T-azido, we used $\epsilon_{265} = 8100\ M^{-1}cm^{-1}$ (Dempcy et al., 1995a,b). The hypochromic shifts were calculated from the absorbances at the extreme temperatures ($A_{260}^{95°C} - A_{260}^{5°C}/A_{260}^{95°C}$).

All experiments were conducted in 10^{-2} M phosphate buffer at pH 7.0, and the ionic strength, μ, was adjusted with KCl and was presented with the corresponding concentration of KCl. The concentrations of nucleosides, expressed in molarity per base, were 2.1×10^{-5}−6.3×10^{-5} M, and the ionic strength $\mu = 0.06$−0.24. The concentration is referred to the limiting component forming the triplex (*e.g.,* a concentration of 2.1×10^{-5} M/base in the reaction of A + 2T means [A] = 2.1×10^{-5} M/base and [T] = 4.2×10^{-5} M/base). All stock solutions were kept at 4 °C between experiments.

Sample Preparation. Five magnetically stirred screw-cap cuvettes of 1 cm path length were used for data collection, four with samples to be measured and one for the temperature monitoring. A layer of Sigmacote (Sigma) was placed above

Scheme 1

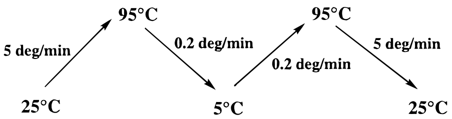

the aqueous reaction solution in order to prevent evaporation, and the measurement chamber was purged continuously with dry nitrogen to prevent condensation of water vapor at lower temperatures. Annealing and melting were followed spectrophotometrically at given wavelengths. For the melting studies of $G_2A_3G_3A_3G_2$ alone at high concentrations, 0.1 cm path length cuvettes were used.

UV Spectroscopy and Data Collection. A Cary 1E UV−vis spectrophotometer equipped with temperature programming and regulation and a thermal melting software package were used for data collection at $\lambda = 260$ nm. Spectrophotometer stability and λ alignment were checked prior to initiation of each melting point experiment. For the T_m determinations, the hypochromicity was used. We considered a well-defined T_m to be within ±1 °C. Data were recorded every 1.0 °C. The samples were heated from 25−95 °C at 5 deg/min (Scheme 1), the annealing (95−5 °C) and the melting (5−95 °C) were conducted at 0.2 deg/min, and the samples were brought back to 25 °C at a rate of 5 deg/min. The reaction solutions were equilibrated for 15 min at the highest and lowest temperatures.

Analysis of Kinetic and Thermodynamic Data for Triplex Formation. The equation for triplex formation that was employed (Rougée et al., 1992) (eq 1) describes the formation of the triplex (Tr) from the duplex (D) and the monomer (M) as individual strands. This equation could be interpreted

$$\mathrm{D} + \mathrm{M} \underset{k_{\mathrm{off}}}{\overset{k_{\mathrm{on}}}{\rightleftharpoons}} \mathrm{Tr}$$

$$K_{\mathrm{eq}} = \frac{k_{\mathrm{on}}^T}{k_{\mathrm{off}}^T} \tag{1}$$

as the reaction of double strand D with single strand M. The expression of kinetic equations for the reactants and products (eq 2) can only be accomplished by expressing the concentrations of strands in molar per base (M/base). The theory

$$\frac{\mathrm{d}[\mathrm{D}]}{\mathrm{d}t} = k_{\mathrm{off}}^T[\mathrm{Tr}] - k_{\mathrm{on}}^T[\mathrm{D}][\mathrm{M}] \tag{2}$$

behind the on and off rates of the dissociation/association of the triplexes and the derivation of kinetic equations has been described in detail (Rougée et al., 1992). In eq 1, a triplex is formed from and dissociates to a duplex and a third monomer strand with rate constants k_{on} and k_{off}. Letting $D_{\mathrm{tot}} = [\mathrm{D}] + [\mathrm{Tr}]$ and $M_{\mathrm{tot}} = [\mathrm{M}] + [\mathrm{Tr}]$, where the subscript tot stands for the total concentration and superscript T stands for temperature, the associated rate for this reaction is given in eq 2. The monitored absorbance is a weighted combination of the absorbances of the trimer, dimer and monomer (eq 3), where $\alpha = [\mathrm{Tr}]/D_{\mathrm{tot}}$.

$$A = \alpha A_{\mathrm{Tr}} + (1-\alpha)A_{D+M} \tag{3}$$

If one defines $\rho = M_{\mathrm{tot}}/D_{\mathrm{tot}}$, eq 2 can be written in terms of α and ρ:

$$\frac{\mathrm{d}\alpha}{\mathrm{d}t} = k_{\mathrm{on}}^T M_{\mathrm{tot}}(1-\alpha)\left(1-\frac{\alpha}{\rho}\right) - k_{\mathrm{off}}^T\alpha \tag{4}$$

As mentioned in earlier works (Rougée et al., 1992; Breslauer et al., 1975; Cantor & Schimmel, 1980), the absorbances for the triplex and duplex, A_{Tr} and $A_{\mathrm{D+M}}$, (α =1 and 0, respectively) are very often temperature dependent. In our determinations, all A_{Tr} and A_{D+M} baselines were well defined and the sloping was considered constant with temperature. The data points were recorded every 1.0 °C, therefore, $\mathrm{d}\alpha/\mathrm{d}t \approx \Delta\alpha/\Delta t = (\alpha_{T+1} - \alpha_{T-1})/2$. In our case, we kept the ratio between the duplex and third strand monomer at 1:1 (*i.e.*, $\rho = 1$) and $\Delta T/\Delta t = 0.2$ deg/min = constant for the melting and the cooling processes. To transform eq 4 from a time-dependent into a temperature-dependent equation, both sides should be multiplied by $\mathrm{d}t/\mathrm{d}T$ and one can obtain the working equations for the heating (h) and the cooling (c) processes (eq 5a,b). At equilibrium, both heating and cooling curves coincide satisfying the mathematical condition $\mathrm{d}\alpha/\mathrm{d}t = 0$ (α = fraction of duplex engaged in the triplex). Thus, from eq 4, $k_{\mathrm{on}}^T \mathrm{M}_{\mathrm{tot}}(1-\alpha)(1-\alpha/\rho) - k_{\mathrm{off}}^T\alpha = 0$. For the cooling curve, $\mathrm{d}T/\mathrm{d}t < 0$ (we are decreasing the temperature) and $\mathrm{d}\alpha/\mathrm{d}t > 0$ (more triplexes are formed in time while cooling; consequently, $\mathrm{d}\alpha/\mathrm{d}T < 0$). Therefore, the right side of eq 4 $[k_{\mathrm{on}}^T \mathrm{M}_{\mathrm{tot}}(1-\alpha)(1-\alpha/\rho) - k_{\mathrm{off}}^T\alpha]$ is positive and the cooling curve is above the equilibration curve. The opposite is valid for the heating curve. If the rate of heating/cooling is smaller than the rate of association or dissociation, there is no hysteresis and the heating and cooling curves coincide to provide the equilibrium curve.

$$\frac{\mathrm{d}\alpha_{\mathrm{h}}^T}{\mathrm{d}T} = \left(\frac{\mathrm{d}T}{\mathrm{d}t}\right)^{-1}\left\{k_{\mathrm{on}}^T M_{\mathrm{tot}}(1-\alpha_{\mathrm{h}})\left(1-\frac{\alpha_{\mathrm{h}}}{\rho_{\mathrm{h}}}\right) - k_{\mathrm{off}}^T\alpha_{\mathrm{h}}^T\right\} \tag{5a}$$

$$\frac{\mathrm{d}\alpha_{\mathrm{c}}^T}{\mathrm{d}T} = \left(\frac{\mathrm{d}T}{\mathrm{d}t}\right)^{-1}\left\{k_{\mathrm{on}}^T M_{\mathrm{tot}}(1-\alpha_{\mathrm{c}})\left(1-\frac{\alpha_{\mathrm{c}}}{\rho_{\mathrm{c}}}\right) - k_{\mathrm{off}}^T\alpha_{\mathrm{c}}^T\right\} \tag{5b}$$

The rate constants k_{on} and k_{off} are functions of temperature and, therefore, can be expressed as Arrhenius equations:

$$k_{\mathrm{on}}M_{\mathrm{tot}} = k_{\mathrm{on}}^{\mathrm{ref}}M_{\mathrm{tot}} \exp\left\{-\frac{E_{\mathrm{on}}}{R}\left(\frac{1}{T} - \frac{1}{T_{\mathrm{ref}}}\right)\right\} \tag{6a}$$

$$k_{\mathrm{off}}M_{\mathrm{tot}} = k_{\mathrm{off}}^{\mathrm{ref}} \exp\left\{-\frac{E_{\mathrm{off}}}{R}\left(\frac{1}{T} - \frac{1}{T_{\mathrm{ref}}}\right)\right\} \tag{6b}$$

where R = 1.98 cal/mol K, and T_{ref} = any arbitrary temperature. For comparison reasons with other reports (Blaskó et al., 1996; Rougée et al., 1992), we chose T_{ref} = 15 °C. In a plot of $\ln(k_{\mathrm{on/off}})$ *vs* $1/T - 1/T_{\mathrm{ref}}$, the thermodynamic parameters $E_{\mathrm{on/off}}/R$ are obtained as slopes and the kinetic $k_{\mathrm{on}}^{\mathrm{ref}}M_{\mathrm{tot}}$, $k_{\mathrm{off}}^{\mathrm{ref}}$ parameters as intercepts. The variation of the values of α at the limits restrict the use of this model to the transition portion of the sigmoidal curve. As recognized earlier by others (Rougée et al., 1992; Breslauer et al., 1975; Cantor & Schimmel, 1980), the sloping of the baselines and the self-association of the single-stranded oligonucleotides limit the accuracy of the determinations.

Double and triple helix stabilities can be described in terms of the standard free energy ($\Delta G°$) (Marky & Breslauer, 1987), if one knows the standard enthalpy and entropy changes ($\Delta H°$ and $\Delta S°$) for the melting of each nearest-neighbor doublet of base pairs in DNA (Petruska & Good-

Table 1: Kinetic and Activation Parameters for the Triplex Melting of d(pA$_n$pG$_m$) with d(Tg)$_4$-T-azido[a]

10^5conc/ base (M)	μ	$10^2k_{on}^{15}M_{tot}$ (s^{-1}) A$_5$G$_3$A$_5$	GA$_4$G$_3$A$_4$G	G$_2$A$_3$G$_3$A$_3$G$_2$	G$_2$A$_2$G$_5$A$_2$G$_2$
6.3	0.06	2.02	1.17	0.87	0.61
	0.08	1.11	0.91	0.54	0.3
	0.12	0.64	0.54	0.24	0.09
	0.24	0.11	0.03	0.05	0.05
2.1	0.06	1.05	0.64	0.19	
	0.08	0.26	0.3	0.07	
	0.12				
	0.24				

10^5conc/ base (M)	μ	$10^6k_{off}^{15}$ (s^{-1}) A$_5$G$_3$A$_5$	GA$_4$G$_3$A$_4$G	G$_2$A$_3$G$_3$A$_3$G$_2$	G$_2$A$_2$G$_5$A$_2$G$_2$
6.3	0.06	1.07	0.75	1.18	5.03
	0.08	3.55	2.24	0.68	7.36
	0.12	6.14	2.9	2.26	8.6
	0.24	18.5	25.4	9.1	41.1
2.1	0.06	6.79	6.14	15.89	
	0.08	5.29	18.46	32	
	0.12				
	0.24				

10^5conc/ base (M)	μ	E_{on}^{15} (kcal/mol) A$_5$G$_3$A$_5$	GA$_4$G$_3$A$_4$G	G$_2$A$_3$G$_3$A$_3$G$_2$	G$_2$A$_2$G$_5$A$_2$G$_2$
6.3	0.06	−19.8	−16.8	−16.8	−18.2
	0.08	−15.8	−15.8	−14.6	−16.8
	0.12	−20.6	−18.2	−17.8	−15.8
	0.24	−21.8	−5.9	−9.1	−8.9
2.1	0.06	−21.8	−16.8	−20.8	
	0.08	−13.9	−18.8	−13.5	
	0.12				
	0.24				

10^5conc/ base (M)	μ	E_{off}^{15} (kcal/mol) A$_5$G$_3$A$_5$	GA$_4$G$_3$A$_4$G	G$_2$A$_3$G$_3$A$_3$G$_2$	G$_2$A$_2$G$_5$A$_2$G$_2$
6.3	0.06	28.7	28.7	22.8	9.9
	0.08	25.7	26.7	27.3	10.3
	0.12	24.2	26.3	17.8	13.8
	0.24	22.8	16.8	15.8	7.9
2.1	0.06	23.8	26.7	17.8	
	0.08	26.7	20.8	13.9	
	0.12				
	0.24				

[a] Margin of errors: $k_{on}^{15}M_{tot} = \pm 0.3 \times 10^{-2}$ s^{-1}; $k_{off}^{15} = \pm 0.3 \times 10^{-6}$ s^{-1}; E_{on}^{15} and $E_{off}^{15} = \pm 0.5$ kcal/mol.

man, 1995). The thermodynamic parameters can be extracted from the kinetic data or can be experimentally determined by calorimetric methods. In many cases, these data obtained by different methods are in good agreement (Albergo et al., 1981). However, at high NaCl concentrations, Howard and co-workers obtained different results for T_m, by using DSC, CD, and UV methods, each of these methods following a particular property of the DNA complexes during melting (Howard et al., 1995).

Equation 7 shows the relationship between the thermodynamic parameters $\Delta H°$ and $\Delta S°$ and the equilibrium constant K_{eq} at a given temperature.

$$\Delta H° - T\Delta S° = -RT \ln K_{eq}(T) \qquad (7)$$

At the melting temperature, T_m, $K_{eq} = 2/M_{tot}$ (Rougée et al., 1992) and at a reference temperature K_{eq} is given by $k_{on}^{ref}/k_{off}^{ref}$. From eq 7, one can calculate the standard molar entropies for the triplex formation and from eq 8 the free energies of formation, $\Delta G°$ (Table 2).

$$\Delta G° = \Delta H° - T\Delta S° \qquad (8)$$

Data Analysis. The Cary 1E data were exported in ASCII format and smoothed in Mathlab (The MathWorks, Inc., Natick, MA) and imported in Mathcad Plus 5.0 (MathSoft, Inc., Cambridge, MA) for calculations and analysis.

RESULTS

Stoichiometry of the Binding. The length of d(Tg)$_4$-T-azido differs from the DNA oligomers in study, and therefore, the triplexes will form in a "domino" fashion (Chart 2, shown for A$_5$G$_3$A$_5$) as previously reported (Blaskó et al., 1996). To accomodate the difference in the strand lengths the concentrations were expressed per mole of nucleotide (Materials and Methods) and the Job plots (continuous variation method) were constructed accordingly. Job plots where constructed from absorbances of solutions containing d(Tg)$_4$-T-azido and the DNA oligomers (A$_5$G$_3$A$_5$, GA$_4$G$_3$A$_4$G, G$_2$A$_3$G$_3$A$_3$G$_2$, and G$_2$A$_2$G$_5$A$_2$G$_2$) in order to establish the stoichiometry of binding. Equilibrated solutions were examined at 10 and 20 °C. The linear dependence of the absorbances *vs* percent T clearly establishes a minima at ca. 67% d(Tg)$_4$-T-azido, which corresponds to the formation of a 2:1 [d(Tg)$_4$-T-azido]$_2$•(DNA) complex (Figure 1). However, there is another break in the Job plots at about 30% T with a small hypochromic shift of <10%. At 10 °C, the curves are well defined, whereas at 20 °C the plots are somewhat shallow such that it is more difficult to define the intersection point of the sloping lines. The hypochromic shift of the [d(Tg)$_4$-T-azido]$_2$•d(A$_5$G$_3$A$_5$) complex is 32% greater than the hypochromic shift of the [d(Tg)$_4$-T-azido]$_2$•d(G$_2$A$_2$G$_5$A$_2$G$_2$) complex.

Hypochromicity on Triplex Formation. By recording the change in absorbance at 260 nm of the [d(Tg)$_4$-T-azido]$_2$ + d(pA$_n$pG$_m$) mixtures between 5 and 95 °C, one can define the hypochromic shift as $A_{260}^{95°C} - A_{260}^{5°C}/A_{260}^{95°C}$. The hypochromic shifts accompanying [d(Tg)$_4$-T-azido]$_2$•d(pA$_n$pG$_m$) triplex formation are between 0.13 and 0.66 in the concentration range of $2.1-6.3 \times 10^{-5}$ M/base and $\mu = 0.06-0.24$ (see Supporting Information). In all cases, greater hypochromic shifts were found for the GA$_4$G$_3$A$_4$G than for A$_5$G$_3$A$_5$. As the G content, increases from GA$_4$G$_3$A$_4$G to G$_2$A$_3$G$_3$A$_3$G$_2$ and G$_2$A$_2$G$_5$A$_2$G$_2$, the decrease in hypochromic shift becomes greater with increase in ionic strength.

Melting Curves at 260 nm and Their Hysteresis Behavior at the Ratios of T:(A,G) of 2:1. We have found that all melting curves exhibit hysteresis (Figure 2). With the increase of the number of mismatches (from A$_5$G$_3$A$_5$, GA$_4$G$_3$A$_4$G, and G$_2$A$_3$G$_3$A$_3$G$_2$ to G$_2$A$_2$G$_5$A$_2$G$_2$), the melting curves become shallow and there can be detected a second transition at around 70−75 °C (Figure 2b). This second transition also exhibits hysteresis behavior. The complexation of d(Tg)$_4$-T-azido with G$_2$A$_2$G$_5$A$_2$G$_2$ is so weak that no T_m values could be located even at 6.3×10^{-5} M/base for the whole range of the ionic strength studied. The shallow hysteresis curve at 6.3×10^{-5} M/base indicates some weak association. At 2.1×10^{-5} M/base, neither T_m nor hysteresis curves could be detected. As the rate of heating and cooling is increased, the rate of equilibration of the species lags such that the hysteresis becomes more marked (Figure 2). These features are shared in the melting characteristics of triplex DNA (Rougée et al., 1992; Maher et al., 1990). The four ramps depicted in Scheme 1 can be visualized in Figure 2 as the variation of the absorbance (A_{260}) *vs* temperature. The gap in the hysteresis curve at a heating/

Table 2: Thermodynamic Parameters for the Triplexes of $A_5G_3A_5$, $GA_4G_3A_4G$, and $G_2A_3G_3A_3G_2$ with d(Tg)$_4$-T-azido

μ	d(pA$_n$pG$_m$)	10^5conc/base (M)	$\Delta H°(288)^{a,b}$ (kcal/mol)	$\Delta S°$ ^{c} (cal/mol K)	$\Delta G°(288)^d$ (kcal/mol)	T_m^{e} (°C)
0.06	$A_5G_3A_5$	6.3	−48.5	−128	−11.8	54.4
		2.1	−45.6	−120	−11.1	46.8
	$GA_4G_3A_4G$	6.3	−45.5	−119	−11.3	53.5
		2.1	−43.3	−113	−10.7	45.6
	$G_2A_3G_3A_3G_2$	6.3	−39.6	−101	−10.4	52; 68[f]
		2.1	−38.6	−99	−10.1	44.2
0.08	$A_5G_3A_5$	6.3	−41.5	−107	−10.7	52.0
		2.1	−40.6	−105	−10.5	45.8
	$GA_4G_3A_4G$	6.3	−42.5	−110	−10.7	51.6
		2.1	−39.6	−103	−10.0	42.1
	$G_2A_3G_3A_3G_2$	6.3	−41.9	−109	−10.6	51; 68[f]
		2.1	−27.4	−65	−8.7	39.3
0.12	$A_5G_3A_5$	6.3	−44.8	−119	−10.5	47.4
		2.1				37
	$GA_4G_3A_4G$	6.3	−44.5	−119	−10.3	46.4
		2.1				36
	$G_2A_3G_3A_3G_2$	6.3	−35.6	−91	−9.4	46; 62[f]
0.24	$A_5G_3A_5$	6.3	−44.6	−122	−9.3	38.8
	$GA_4G_3A_4G$	6.3	−22.7	−53	−7.5	36.2

[a] From $E_{on} - E_{off}$5. [b] ±0.2 kcal/mol. [c] ±1 cal/mol K. [d] ±0.3 kcal/mol. [e] ±1 °C. [f] Second transition.

Chart 2

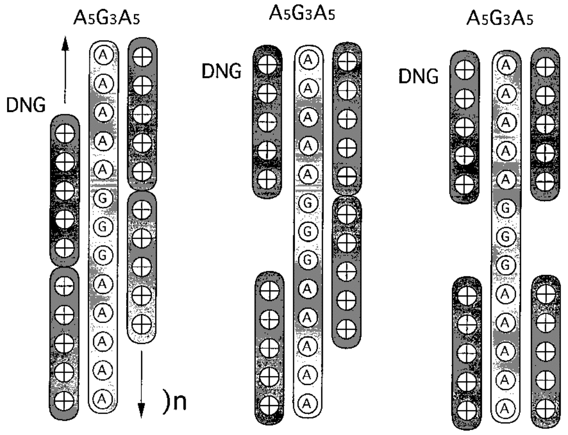

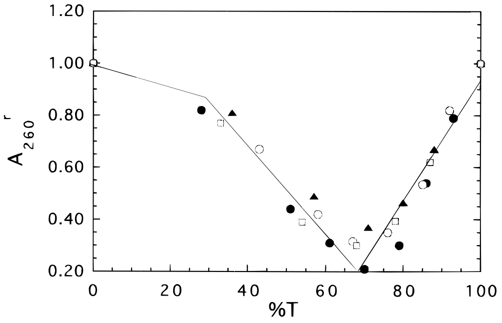

FIGURE 1: Job plot (continuous variation method) of $A_5G_3A_5$ (●), $GA_4G_3A_4G$ (○), $G_2A_3G_3A_3G_2$ (▲), and $G_2A_2G_5A_2G_2$ (□) with d(Tg)$_4$-T-azido at 6 × 10^{-5} M/base total concentration of DNG and DNA, at λ = 260 nm and 10 °C. $A^r_{260} = A_i/(A_{DNG}x_{DNG} + A_{DNA}x_{DNA})$. Two breaks can be detected at ca. 30 and 67% T. Between 0 and 30% T there is little change in the absorbance.

cooling rate of 5 deg/min (first and the fourth ramps) is larger than at a heating/cooling rate of 0.2 deg/min (the second and the third ramp).

Effect of the Ionic Strength on T_m. At the concentration of 2.1 × 10^{-5} M/(base T) and a 2:1 ratio between the T bases and DNA bases (in 10^{-2} M phosphate buffer, pH 7.0) we saw only one T_m transition (at 260 nm) after annealing d(Tg)$_4$-T-azido with $A_5G_3A_5$, $GA_4G_3A_4G$, and $G_2A_3G_3A_3G_2$ (Figure 3). We assigned this transition to the triplex denaturation. With increase in ionic strength (μ), the value of T_m decreases (Figure 3). Regardless of the source of dA (*i.e.*, $A_5G_3A_5$, $GA_4G_3A_4G$, and $G_2A_3G_3A_3G_2$), the slope of a plot of T_m *vs* μ equals ca. −100 deg/(unit of ionic strength) at a concentration of 6.3 × 10^{-5} M/base. However, small differences in the slope can be observed at higher degree of mismatched base pairs and at a concentration of 2.1 × 10^{-5} M/base (Figure 3). Above μ = 0.12, the melting curves become shallow (*i.e.*, ΔA_{260} becomes smaller) and the T_m determination is less accurate. At the concentration of 2.1 × 10^{-5} M/base, the highest ionic strength where we could determine the T_m values was 0.12.

Rate Constants and Activation Energies. The expression which provides the temperature dependence of the rate constants for association (k_{on}) and dissociation (k_{off}) is provided in eq 6. At a given reference temperature eq 6 provides k^{ref}_{on} and k^{ref}_{off} as well as the activation E_{on} and E_{off} parameters (Figure 4). Inspection of Table 1 shows that the values of k_{on} at 288 K are between 10 and 500 M^{-1} s^{-1} and the values of k_{off} at 288 K are between 10^{-6} and 40 × 10^{-6} s^{-1}. The energies of activation E_{on} at 288 K were between −9 and −22 kcal/mol and E_{off} at 288 K, between 8 and 29 kcal/mol.

By decreasing the ionic strength, k_{on} increases, while k_{off} decreases (Figures 5 and 6). The variation of k_{on} and k_{off} is found to be exponential with change of ionic strength. For $A_5G_3A_5$ at 6.3 × 10^{-5} M/base concentration using 15 °C as T_{ref}, $\Delta k_{on}M_{tot}$ = 1.9 × 10^{-2} s^{-1} and Δk_{off} = 34 × 10^{-6} s^{-1}. With the ionic strength decrease (0.24 to 0.06), E_{on} decreases from −20 to −22 kcal/mol, whereas E_{off} increases from 10 to 14 kcal/mol (Table 1).

At μ = 0.06, an increase in $A_5G_3A_5$ concentration from 2.1 × 10^{-5} M/base to 6.3 × 10^{-5} M/base, while maintaining the 2:1 ratio of T:(A,G), results in an increase in $k^{15}_{on}\cdot M_{tot}$ [$k^{15}_{on} \approx 400$ M^{-1} s^{-1} (molarity in per base T)], whereas k^{15}_{off} has scattered values (with a tendency to higher values at lower concentrations) (Table 1). No significant dependence of E_{on} and E_{off} on the DNA mismatches was found in the DNA concentrations and the ionic strength range studied.

At the higher concentration of the components forming triplexes (*e.g.*, 6.3 × 10^{-5} M/base) and μ = 0.06, the dependence of k^{15}_{on} and k^{15}_{off} upon the number of mismatched base pairs is exponential. For $A_5G_3A_5$, $GA_4G_3A_4G$, $G_2A_3G_3A_3G_2$, and $G_2A_2G_5A_2G_2$, the values of $k^{15}_{on}\cdot M_{tot}$ de-

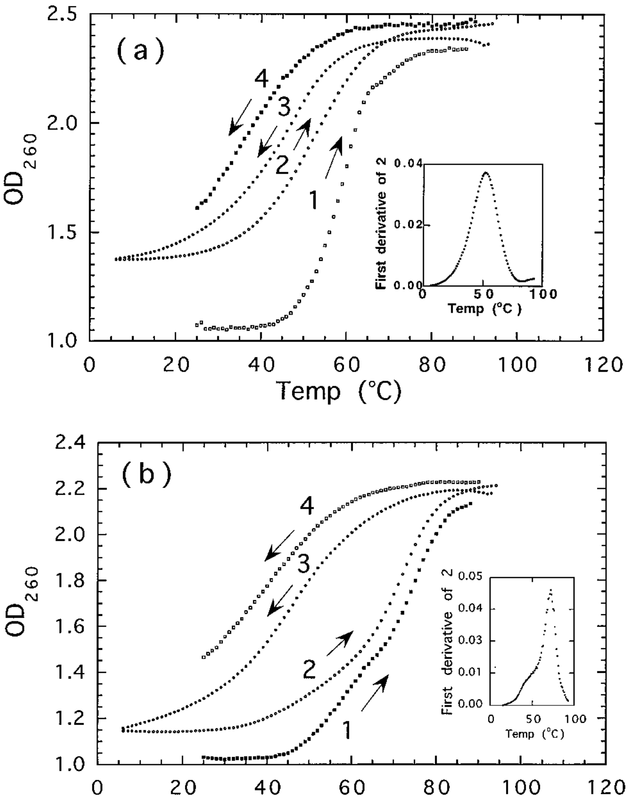

FIGURE 2: Effect of the heating/cooling rate on the extent of association/dissociation of the triplex of $A_5G_3A_5$ (Figure 2a) and $G_2A_3G_3A_3G_2$ (Figure 2b) with d(Tg)$_4$-T-azido at 6.3×10^{-5} M/base monomer concentration and $\mu = 0.08$. (1) fast heating (5 deg/min); (2) slow melting (0.2 deg/min); (3) slow annealing (0.2 deg/min); (4) fast cooling (5 deg/min). The second transition in the hysteresis curve (b) was assigned to a fold-back structure of $G_2A_3G_3A_3G_2$ assisted by d(Tg)$_4$-T-azido. After the dissociation of one of the d(Tg)$_4$-T-azido strands from $G_2A_3G_3A_3G_2$, there is a folding back of the 13-mer oligonucleotide to which d(Tg)$_4$-T-azido binds as a third strand and this dissociates at higher temperature (see text and Chart 2, middle, and Scheme 2).

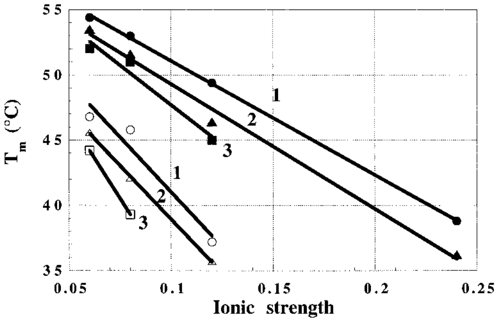

FIGURE 3: Dependence of the T_m on ionic strength (μ) for the dissociation of triplex formed between d(Tg)$_4$-T-azido and $A_5G_3A_5$ (1), $GA_4G_3A_4G$ (2), and $G_2A_3G_3A_3G_2$ (3) at 6.3×10^{-5} M/base (solid symbols) and 2.1×10^{-5} M/base (open symbols). No T_m determination was possible at these concentrations for $G_2A_2G_5A_2G_2$ (see text and Table 2). With the increase in the G content (mismatched base pairs) at a certain concentration (e.g., 6.3×10^{-5} M/base) discrimination (change in fidelity) occurs in the formation and strength of binding of d(Tg)$_4$-T-azido to d(pA$_n$pG$_m$) oligomers.

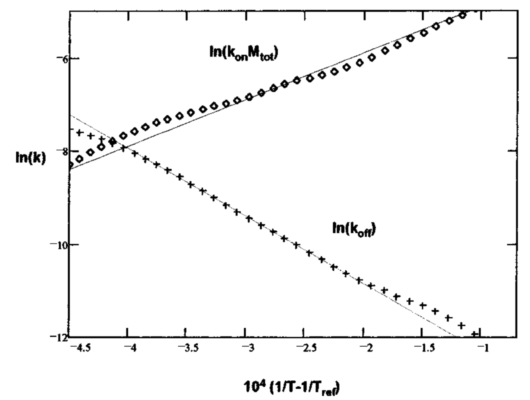

FIGURE 4: Dependence of $\ln(k_{\text{on}}M_{\text{tot}})$ and $\ln(k_{\text{off}})$ on $1/T$ for the denaturation/renaturation of triplex of [d(Tg)$_4$-T-azido]$_2$•d($A_5G_3A_5$) at 6.3×10^{-5} M/base and $\mu = 0.06$ and dT/dt = 0.2 deg/min.

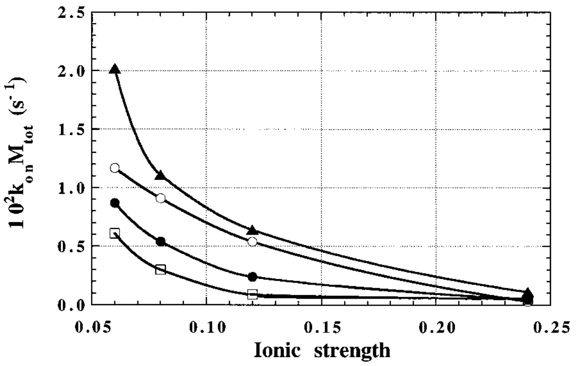

FIGURE 5: Dependence of $k_{\text{on}}^{15°\text{C}}$ on ionic strength for denaturation/renaturation of the triplexes formed from $A_5G_3A_5$ (▲), $GA_4G_3A_4G$ (○), $G_2A_3G_3A_3G_2$ (●), and $G_2A_2G_5A_2G_2$ (□) (6.3×10^{-5} M/base) with d(Tg)$_4$-T-azido (12.6×10^{-5} M/base) at dT/dt = 0.2 deg/min.

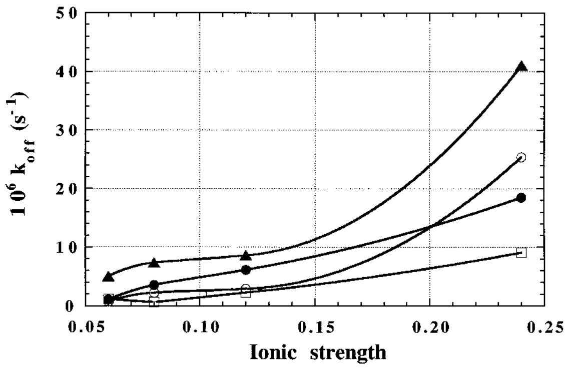

FIGURE 6: Dependence of $k_{\text{off}}^{15°\text{C}}$ on ionic strength for denaturation/renaturation of the triplexes formed from $A_5G_3A_5$ (●), $GA_4G_3A_4G$ (○), $G_2A_3G_3A_3G_2$ (□), and $G_2A_2G_5A_2G_2$ (▲) (6.3×10^{-5} M/base) with d(Tg)$_4$-T-azido (12.6×10^{-5} M/base) at dT/dt = 0.2 deg/min.

crease with increase in the G content of the DNA oligomers whereas k_{off}^{15} increases (Figure 7). The E_{on} values are negative and become generally less negative with the increase in the G content of the DNA oligomers, while the E_{off} values are positive and decrease with the increase in the G content of the DNA oligomers. The $\Delta H°$ values ($\Delta H° = E_{\text{on}} - E_{\text{off}}$) are negative and become less negative with the increase in the G content of the DNA oligomers.

DISCUSSION

Using thermal equilibration and melting analysis, we have previously shown (Blaskó et al., 1996) that the d(Tg)$_4$-T-azido polycation binds to short strand d(pA)$_x$ oligomers (x = 5−18) with unprecedented affinity to provide triple-stranded helices. With poly(dA), we saw both double- and triple-stranded complexes, but only with triple helices does one observe hysteresis behavior (Dempcy et al., 1995a; Blaskó et al., 1996). Further, we find that the well studied

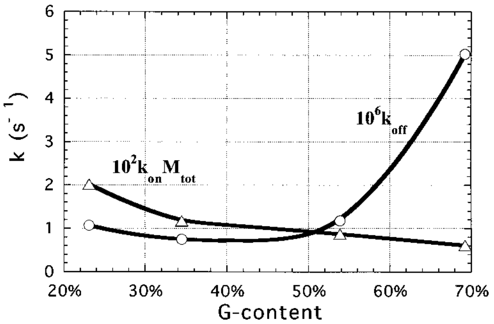

FIGURE 7: Dependence of $k_{on}^{15°C}$ and $k_{off}^{15°C}$ on the percent G content of $A_5G_3A_5$, $GA_4G_3A_4G$, $G_2A_3G_3A_3G_2$, and $G_2A_2G_5A_2G_2$ at 6.3×10^{-5} M/base concentration and $\mu = 0.06$. Note the difference in the order of magnitude of k_{on} and k_{off}.

increase in T_m with increase in ionic strength (μ) on the reaction of DNA with DNA or RNA is reversed in the interaction of d(Tg)$_4$-T-azido with d(pA)$_x$ such that T_m is increased with decrease in μ. The effect of μ in the reaction of d(Tg)$_4$-T-azido with d(pA)$_x$ is the more pronounced. Increasing ionic strength attenuates the electrostatic interactions between strands [electrostatic forces are repulsive between negatively charged DNA and RNA oligomers and attractive between positively charged d(Tg)$_4$-T-azido and negatively charged DNA or RNA]. Thus, the reaction of d(Tg)$_4$-T-azido with DNA or RNA is favored at physiologic ionic strength whereas the complexing of DNA by DNA or RNA is not so favored.

Stoichiometry of Binding. Knowledge of the stoichiometry of binding must be available prior to any investigation of denaturation/renaturation. The continuous variation method (Job plots) is commonly used to establish the ratio between components forming complexes in solution. Job plots constructed from absorbances of solutions containing d(Tg)$_4$-T-azido and the DNA oligomers ($A_5G_3A_5$, $GA_4G_3A_4G$, $G_2A_3G_3A_3G_2$, and $G_2A_2G_5A_2G_2$) clearly established a minima at ca. 67% T which corresponds to the formation of a [d(Tg)$_4$-T-azido]$_2$•(DNA) complex (Figure 1). There is a second break in the Job plots at about 30% T, which denotes that another complex forms at a 1:2 ratio between Ts and DNA bases. Such unusual structures are not uncommon in the DNA−DNA interactions where two purines form triplexes with one pyrimidine (PyPuPu triple helices). While no direct experimental evidence exists for polarity of the third strand in the TAA case, there is evidence for analogous triple helices with mixed CT sequences paired (WC) to AG strands and a third strand of A and G paired (A to A; G to G, with AA interactions being weaker than GG interactions) to the original WC purine strand (Howard et al., 1995). The PyPuPu motif is found in the DNA nonamer d(GCGAATTCG) characterized by X-ray diffraction at 2.05 Å resolution (Van Meervelt et al., 1995). The extended crystal structure contains (C•G)*G triplets as a fragment of triple helix with the guanosine containing chains in a parallel orientation. The first intersection point in the Job plots is below 33% T (Figure 1) that would correspond to the 1:2 ratio between Ts and DNA bases. This phenomenon of lowering of the intersection points in the Job plots has been seen when odd bases are looping out. Pentamers and hexamers of the general formula A$_n$G and GA$_n$ and poly(U) form triplexes with the odd bases close for looping out (*i.e.*, the odd bases are outside) and their mixing curves exhibit an intersection point less than 66.7% poly(U) (Uhlenbeck & Harrison, 1968). However, the location of the noncomplementary nucleotide at the 5′ end of the oligomer chain leads to greater stability and greater hypochromicity.

Hypochromic Shifts. The hypochromic shift of the [d(Tg)$_4$-T-azido]$_2$•d($A_5G_3A_5$) complex (Blaskó et al., 1996) is 32% greater than the hypochromic shift of the [d(Tg)$_4$-T-azido]$_2$•d($G_2A_2G_5A_2G_2$) complex showing that with the increase in the number of mismatched base pairs the association in triplexes is weaker and weaker (Figure 1). The fact that $GA_4G_3A_4G$ is associated with a higher hypochromic shift than $A_5G_3A_5$ while forming triplexes with d(Tg)$_4$-T-azido is consistent with the stabilization effect brought about by the end G noncomplementary bases (Uhlenbeck & Harrison, 1968) (*vide supra*). With the increase in the G content of the oligonucleotides and ionic strength, the hypochromic effect is lower and lower showing more and more destabilization of the triplexes in solution. Quantitative treatment of this observation comes from the melting experiments (*vide infra*).

Melting Studies. By inspection of Figure 3, the plot of T_m *vs* μ [for d(Tg)$_4$-T-azido complexes with $A_5G_3A_5$, $GA_4G_3A_4G$, and $G_2A_3G_3A_3G_2$, T:(A,G) 2:1] has a slope of ca. −100 deg/(unit of ionic strength) which is 2 times larger than in the case of d(Tg)$_4$-T-azido interacting with short strand DNA homooligomers (Blaskó et al., 1996). This relatively large value is a measure of the pronounced ionic strength effect on T_m and also shows that with the incorporation of mismatched base pairs the binding is weaker. Although at higher concentration of the components (*e.g.*, 6.3×10^{-5} M/base) the decrease in the T_m values with μ is practically not affected by the number of mismatched base pairs, at lower concentrations (*e.g.*, 2.1×10^{-5} M/base) there is a differentiation in the sloping of the plot of T_m *vs* μ (Figure 3). Due to the accuracy of the determinations at low concentrations of the components forming triplexes, the increase in the negative value of the sloping lines between $A_5G_3A_5$ and $G_2A_2G_5A_2G_2$ can only be estimated to be by a factor of 2. The effect of ionic strength is also seen on inspection of the melting plots. As the ionic strength is increased above $\mu = 0.08$, the melting curves are shallow and ΔA_{260} becomes smaller and smaller showing that the equilibrium constant for the triplex formation decreases with the increase in μ. By inspection of Figure 3, at 2.1×10^{-5} M/base concentration the T_m values could be determined only at $\mu < 0.12$ (*i.e.*, lower than the physiological ionic strength). At higher concentrations (*e.g.*, 6.3×10^{-5} M/base), one can differentiate between the four mismatched triplexes. In the range of physiological ionic strength (0.15−0.30) and below, $A_5G_3A_5$ and $GA_4G_3A_4G$ have well-defined T_m values which, of course, decrease with μ. However, $G_2A_3G_3A_3G_2$ and $G_2A_2G_5A_2G_2$ do not have well-defined T_m values above $\mu = 0.12$! Their melting curves are very shallow and their hypochromic shifts are small denoting negligible binding at physiological ionic strength. Therefore, with the increase in the G content (mismatched base pairs) at a certain concentration (*e.g.*, 6.3×10^{-5} M/base) discrimination (change in fidelity) occurs in the formation and strength of binding of d(Tg)$_4$-T-azido to d(pA$_n$pG$_m$) oligomers.

The divergence of the heating and cooling curves are functions of the rates of heating and cooling and is greater at 5 deg/min than at 0.2 deg/min. With the increase in the number of mismatches (percent G: $A_5G_3A_5 < GA_4G_3A_4G < G_2A_3G_3A_3G_2 < G_2A_2G_5A_2G_2$), the melting curves are shallow and there is detected a second transition at around 70−75 °C at a concentration of 6.3×10^{-5} M/base (Figure

2b). This could not be detected at 2.1×10^{-5} M/base. This second transition on the melting curve is weaker with $GA_4G_3A_4G$ than with $G_2A_3G_3A_3G_2$. At higher G content (*e.g.*, $G_2A_2G_5A_2G_2$), however, due to very little association with d(Tg)$_4$-T-azido in the range of $\mu = 0.06-0.24$, the melting points with $G_2A_2G_5A_2G_2$ could not be determined. This weak association at a concentration of 6.3×10^{-5} M/base of $G_2A_2G_5A_2G_2$ is supported by the inability to observe hysteresis in the heating/cooling curves at 2.1×10^{-5} M/base.

G−G Interactions. The G-rich sequences and mismatched base pairs are very important in biological events, however, their biophysical characterization is not so easy. All our studied oligonucleotides are G-rich sequences and they differ not only in the G content but also in the base sequence (*e.g.*, $A_5G_3A_5$ *vs* $GA_4G_3A_4G$).

Our observed second T_m transition in the case of the G-rich oligomer $G_2A_3G_3A_3G_2$ has to be addressed. Previously, we saw two T_m transitions with poly(dA) but only with the first transision (the triplex denaturation) does one observe hysteresis behavior (Dempcy et al., 1995a; Blaskó et al., 1996). Also, the second transition has a much smaller hypochromic shift. With short strand DNA oligomers, we saw only one transition with hysteresis. On the basis of these observations, our observed second T_m transition in the case of $G_2A_3G_3A_3G_2$ (Figure 2b) cannot be attributed to the duplex denaturation. Self-association of G-rich sequences are not uncommon in quadruplexes (Sen & Gilbert, 1990; Balagurumoorthy & Brachmachari, 1994; Olivas & Maher, 1995; Jin et al., 1992; Mergny et al., 1995), hairpins (Balagurumoorthy & Brachmachari, 1994), three-way junctions (Hüsler & Klump, 1994), costack intercalations (Chou et al., 1994), polymeric duplexes (Jaskunas et al., 1969), or fold-back structures (Hirao et al., 1994; Vo et al., 1995; Plum & Breslauer, 1995). Single-stranded DNA containing short guanine-rich motifs as in the case of our $G_2A_3G_3A_3G_2$ will self-associate at physiological salt concentrations to make four-stranded structures in which the strands run in parallel fashion. The melting temperature, for $d(TG_3T)_2,K^+$ is 65 °C at 0.5 deg/min (Jin et al., 1992), which is ca. 10 °C lower than our second transition (70−75 °C at 0.2 deg/min, Figure 2b) when comparing the 10-mer, $d(TG_3T)_2$, with our 13-mer, $G_2A_3G_3A_3G_2$.

Other possible structures that may be derived from our $G_2A_3G_3A_3G_2$ are fold-back structures with either G or A in the loop and the third strand fulfilled by Ts from d(Tg)$_4$-T-azido. It was shown by ^{1}H NMR spectroscopy that d(GCGAAGC) is folded back on itself between A_4 and A_5, and all the sugars in the fragment adopt the C-2′-*endo* conformation (Hirao et al., 1994). Further, the T_m of the folded-back d(GCGAAGC) is 76 °C. This value is within the range of our second transition in the melting of [d(Tg)$_4$-T-azido]$_2$·d($G_2A_3G_3A_3G_2$) triplex (Figure 2b).

Another possibility of self-association of our $G_2A_3G_3A_3G_2$ is by aggregation in polymeric duplexes. It was shown that self aggregation is also accompanied by a hypochromic effect (Jaskunas et al., 1969).

In order to differentiate between self-aggregation and unusual associations induced by d(Tg)$_4$-T-azido, we have performed melting experiments with $G_2A_3G_3A_3G_2$ alone under the same experimental conditions where we found the second transition in the melting curves in the presence of d(Tg)$_4$-T-azido. By recording the melting curves (annealing and heating), we found no transitions between 5 and 95 °C in the range of the $G_2A_3G_3A_3G_2$ concentrations of $2.1-6.3 \times 10^{-5}$ M/base (our experimental conditions), only a small sloping of the base line (0.1 o.d. change). The cooling curve at 6.3×10^{-5} M/base exhibits a transition at ca. 85 °C with an o.d. change of 0.3 absobtion unit. This could correspond to a transition in the melting curve of >100 °C. At 12.6×10^{-5} M/base and 19.0×10^{-5} M/base, there was observed bigger sloping up of the base lines and the cooling curves exhibit transitions at 90 and 95 °C (data not shown). The shape of the melting curves and the estimated transition temperatures are those characteristic of quadruplex melting profiles (Jin et al., 1992). However, the small o.d. change is not consistent with the formation of a significant ammount of self associated complexes (*e.g.*, quadruplexes). This observation excludes significant self aggregation for the concentration range of $2.1-6.3 \times 10^{-5}$ M/base, but does not rule out the possibility of formation of the three types of structures (*vide supra*) assisted by d(Tg)$_4$-T-azido. We consider that in our case $G_2A_3G_3A_3G_2$ is likely to form a fold-back structure assisted by d(Tg)$_4$-T-azido (Scheme 2).

Scheme 2

After the triplex melting, the duplex containing $G_2A_3G_3A_3G_2$ and Ts folds back on the 13-mer with concomitent loss of d(Tg)$_4$-T-azido (Scheme 2). The Pu-Pu-Py fold-back structure dissociates at higher temperature than the Py-Pu-Py triplexes.

The ratio between the pyrimidines of d(Tg)$_4$-T-azido and the purines of the DNA is 1:2. This 1:2 stoichiometry has been established by continuous variation experiments (Figure 1, first break). In the case of the oligonucleotide $G_2A_2G_5A_2G_2$, there are not enough complementary sites to bind d(Tg)$_4$-T-azido due to the higher content of mismatched base pairs, therefore, no unusual structures (*e.g.*, fold-back structures) assisted by d(Tg)$_4$-T-azido can exist.

Kinetics. The kinetics of the triplex formation and dissociation is described by k_{on} and k_{off} (eq 1). Here and elsewhere (Rougée et al., 1992; Breslauer et al., 1975), species other than full associations are neglected (all-or-none model) in the kinetic and thermodynamic studies. There is little or no sloping of the baseline (Figure 2), and in the concentration range studied the self-association of the single strands is negligible (Vesnaver & Breslauer, 1991). For $G_2A_3G_3A_3G_2$, only the first part of the hysteresis curve, corresponding to the first T_m transition was used for the calculations.

At 15 °C, the second-order rate constants, k_{on}, for triplex formation with $A_5G_3A_5$, $GA_4G_3A_4G$, $G_2A_3G_3A_3G_2$, and $G_2A_2G_5A_2G_2$ are in the range $10-500$ M^{-1} s^{-1} (the molarity is expressed in per base) and the first-order rate constants k_{off} are between 10^{-6} s^{-1} and 40×10^{-6} s^{-1} in the range $\mu = 0.06-0.24$. At T:(A,G) ratio of 2:1, we compare the kinetic parameters of the reaction between d(Tg)$_4$-T-azido with $A_3G_5A_3$ and with d(pA)$_{10}$ (Blaskó et al., 1996). At a concentration of 2.1×10^{-5} M/base and $\mu = 0.08$, we find the values of k_{on} and k_{off} to be comparable (for $A_3G_5A_3$ $k_{on}M_{tot} = 2.6 \times 10^{-3}$ s^{-1}; $k_{off} = 6.8 \times 10^{-6}$ s^{-1} and for d(pA)$_{10}$ $k_{on}M_{tot} = 1.7 \times 10^{-3}$ s^{-1}; $k_{off} = 9.0 \times 10^{-6}$ s^{-1}). The slight difference is ascribed to the difference in the chain length of the DNA oligomers. This comparison shows also that a G content of 23% does not significantly change the strength of the binding of d(Tg)$_4$-T-azido with a 13-mer DNA. The same observation is seen with the activation energies. However, with further increase in the G content, both k_{on}

and k_{off} change dramatically (Figure 7) toward weaker binding. There is a close relationship between the T_{m} values and the kinetic and activation parameters for triplex formation because ultimately they are describing the strength of association. As expected, by decreasing the ionic strength, k_{on} increases, while k_{off} decreases (Figures 5 and 6). As one changes μ, the variation of k_{on} and k_{off} is found to be exponential. At lower G content (*e.g.*, 23%), the triplexes behave similarly to short strand homooligomers [*e.g.*, d(pA)$_{10}$]. With the increase of the G content, the effect of the ionic strength on k_{on} and k_{off} is more marked and, for both constants, there is a 4-fold change from $A_5G_3A_5$ (23% G) to $G_2A_2G_5A_2G_2$ (69% G). The existence of the ionic strength dependence on k_{off} is ascribed to the fact that the electrostatic phenomena are more pronounced in the case of triplexes of d(Tg)$_4$-T-azido with d(pA$_n$pG$_m$) than in the case of DNA triplexes where k_{off} has no ionic strength dependence (Breslauer, 1986).

Clues as to the nature of structure are obtainable from the concentration dependence of the kinetic parameters for triplex formation. At $\mu = 0.06$, the second-order rate constant with $A_5G_3A_5$ ($k_{\mathrm{on}}^{15°\mathrm{C}} \approx 400\ \mathrm{M^{-1}s^{-1}}$, molarity in per base) remains constant on increase in the concentration of reactants by a factor of 3, while maintaining the 2:1 T:(A,G) ratio between d(Tg)$_4$-T-azido and DNA. The increase in k_{off} on decrease in complex concentration (6.3 to 2.1×10^{-5} M/base) is much greater at higher G content of the DNA oligomers. This could be an indication that the dissociation process in the case of G-rich noncomplementary sequences is more complex and could involve intermediary steps.

Activation Energies. With decrease in ionic strength, E_{on} decreases from -20 to -22 kcal/mol, whereas E_{off} increases from 10 to 14 kcal/mol (Table 1). Also, the E_{on} values are negative and become generally less negative with the increase in the G content of the DNA oligomers, while the E_{off} values are positive and decrease with the increase in the G content of the DNA oligomers. The behavior of E_{on} and E_{off} with the change in ionic strength and G content of the oligimers is consistent with a better stabilization of the triplexes at low ionic strength and at low percent G of the DNA oligomers.

Thermal stabilities depend not only on base composition, but also on nucleotide sequence (Breslauer, 1986). This discovery has intensified the interest in thermodynamic data which were needed to interpret the results of kinetic studies on DNA and RNA conformational changes and in defining the nature of the inter- and intramolecular forces that stabilize single- and double-stranded DNA and RNA structures. The variation in stability of short strand triple helices of d(pA)$_x$ homooligomers with d(Tg)$_4$-T-azido fall over a range -8 to -12 kcal/mol (Blaskó et al., 1996). We found that the same range is valid for the triplexes between d(Tg)$_4$-T-azido and mismatched base pairs [d(pA$_n$pG$_m$)] (Table 2); however, the enthalpy−entropy compensation is different (*vide infra*).

Single-stranded DNA, as well as RNA bases, are stacked resembling a single strand of a double helix and they bring their own energy contributions in forming duplexes and triplexes (Cantor et al., 1970), and the actual enthalpies of duplex and triplex formation must reflect the fact that the single strands are already in a helical conformation (Vesnaver & Breslauer, 1991). In many cases, stacking interactions are more important than pairing interactions in determining the stability of the terminal base pairs (Petersheim & Turner, 1983), which in the case of short strand oligonucleotides play a key role. The thermodynamic contribution of the sequence of bases in DNA oligomers to duplex stability is small, and the enthalpies of formation could contain up to 40% of the ssDNA enthalpies that ultimately stabilizes the final duplex state (Vesnaver & Breslauer, 1991). Experimental enthalpies for formation of DNA triplexes from duplexes and single strands range from ca. -2 to -7 kcal/(mol of base) (Wilson et al., 1994).

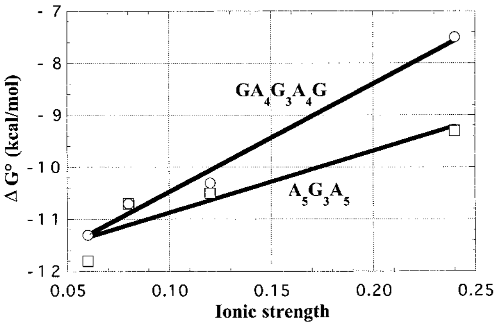

FIGURE 8: Dependence of $\Delta G°$ on ionic strength for the formation of [d(Tg)$_4$-T-azido]$_2$•d($A_5G_3A_5$) and [d(Tg)$_4$-T-azido]$_2$•d($GA_4G_3A_4G$) complexes.

The standard molar enthalpies have larger negative values at low ionic strength than at high ionic strength in accord with the observation that at lower μ values the formation of triplexes of d(Tg)$_4$-T-azido with d(pA$_n$pG$_m$) is more favored. The standard molar enthalpies $\Delta H°(288) = E_{\mathrm{on}} - E_{\mathrm{off}}$ in the range $\mu = 0.06-0.24$ are between -48.5 and -22.7 kcal/(mol base) for [d(Tg)$_4$-T-azido]$_2$•d(pA$_n$pG$_m$) complexes while $\Delta H°(288)$ for [d(Tg)$_4$-T-azido]$_2$•d(pA)$_{5-10}$ complexes are lower [-69 to -27 kcal/(mol base)] (Blaskó et al., 1996). Triplex formation between d(Tg)$_4$-T-azido and $A_5G_3A_5$ is associated with values of $\Delta G°$ ranging between -9.3 and -11.8 kcal/mol with large negative values at low ionic strengths (Table 2 and Figure 8). The $\Delta G°$ values of formation of the [d(Tg)$_4$-T-azido]$_2$•d(pA)$_{5-10}$ triple helices are ca. 20% lower compared to $\Delta G°$ values for the triple helices of [d(Tg)$_4$-T-azido]$_2$•d(pA$_n$pG$_m$). This small difference is attributed to the interaction of the G bases with the noncomplementary bases. Thermal melting analysis demonstrated that the presence of noncomplementary blocks of G−G or G−A mismatches does not disrupt cooperative interactions between flanking regions of G−C base pairs (Modrich, 1987). Further, the G−T wobble pair is accomodated within A, B, or Z-DNA helices with little effect on global helix structure or backbone conformation. However, a greater G content in our d(pA$_n$pG$_m$) oligomers destabilizes the formation of [d(Tg)$_4$-T-azido]$_2$•d(pA$_n$pG$_m$) complex (Table 2). The triplex of d(Tg)$_4$-T-azido with the 13-mer $A_5G_3A_5$ with the lowest G content in the studied DNA oligomers has comparable free energies with the short strand homooligomes binding to d(Tg)$_4$-T-azido. This is consistent with the on and off rates of the denaturation/renaturation processes (Table 1). Neither a low G content significantly changes the strength of binding nor does the replacement of T-G by G-T or G-A by A-G, which yield heteroduplexes differing in free energy by 0.7 to 0.9 kcal/mol at 25 °C (Aboul-ela et al., 1985). It was also shown that, at room temperature, the most stable mismatches in the double-stranded formation for base−base mismatches of the sequence d(CA_3XA_3G)•d(CT_3YT_3G) (with each of the bases A, C, G, and T at the positions labeled X and Y) are those containing guanine (G-T, G-G, G-A) (Aboul-ela et al., 1985).

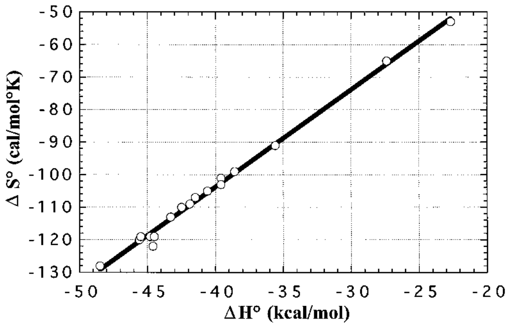

FIGURE 9: Enthalpy−entropy compensation in the [d(Tg)$_4$-T-azido]$_2$·d(pA$_n$pG$_m$) triplex melting thermodynamics.

The neighboring sequence is an important factor in stability, and base stacking is necessary for duplex stability. However, hydrogen bonding may be necessary to allow the bases close enough to each other inside the helix where they can stack. We noticed that the hypochromic shifts of GA$_4$G$_3$A$_4$G while forming triplexes with d(Tg)$_4$-T-azido are greater than those of complexes with A$_5$G$_3$A$_5$ (see Supporting Information). This is reflected in the values of k_{off} (Figure 7) for GA$_4$G$_3$A$_4$G which are lower (better stabilization) than the k_{off} values for A$_5$G$_3$A$_5$ and G$_2$A$_3$G$_3$A$_3$G$_2$. By inspection of Figure 8, the $\Delta G°$ values increase with the increase in percent G. Even with a higher overlap of the bases in the GA$_4$G$_3$A$_4$G triplexes with d(Tg)$_4$-T-azido (greater hypochromic shifts), their $\Delta G°$ values are not lower than the $\Delta G°$ values for A$_5$G$_3$A$_5$ triplexes with d(Tg)$_4$-T-azido (the hydrogen bond interactions at the site of the mismatched base pairs are weaker leading to less stable triplexes). This is valid for short strand DNA oligomers. For DNA fragments of 373 bp long, with two adjacent mismatched base pairs, and eight DNAs with Watson−Crick base pairs at the same positions (studied by temperature-gradient gel electrophoresis, TGGE), the two adjacent G−A pairs, d(CGAG)·d(CGAG), created a more stable DNA than DNAs with Watson−Crick A−T pairs at the same sites (by ca. 0.4 kcal/mol) (Ke & Wartell, 1996), consistent with the unusual stability of the d(GA)·d(GA) sequence previously observed in DNA oligomers (Ebel et al., 1992). The sequence dependent next neighbor stacking interactions influence DNA stability. Thus, it is not surprising that [d(Tg)$_4$-T-azido]$_2$·d(A$_5$G$_3$A$_5$) complex is comparable with [d(Tg)$_4$-T-azido]$_2$·d(pA)$_{10}$ complex regarding their stabilities (Blaskó et al., 1996).

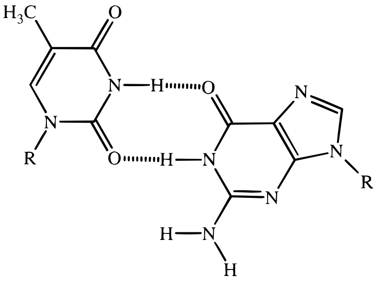

Structure of T-G (Modrich, 1987)

In the formation of [d(Tg)$_4$-T-azido]$_2$·d(pA$_n$pG$_m$) triplex, the value of $T\Delta S°/\Delta H°$ is smaller than for formation of the [d(Tg)$_4$-T-azido]$_2$·d(pA)$_x$ triplex (Blaskó et al., 1996). "Enthalpy-driven" reactions were found in the tetramolecular quadruplex formation of the sequence d(T$_{1-4}$G$_4$) (−22 to −24 kcal/mol of G tetrad) (Pilch et al., 1995). A plot of $\Delta S°$ *vs* $\Delta H°$ shows a linear dependence (Figure 9) and can be related to the enthalpy−entropy compensation earlier reported (Blaskó et al., 1996) (the slope, $\Delta S°/\Delta H° = 0.0026$ K^{-1} for mismatch base pairs and $\Delta S°/\Delta H° = 0.0030$ K^{-1} for homooligomers).

CONCLUSIONS

The d(Tg)$_4$-T-azido polycation binds to short strand G-rich DNA oligomers (A$_5$G$_3$A$_5$, GA$_4$G$_3$A$_4$G, G$_2$A$_3$G$_3$A$_3$G$_2$, and G$_2$A$_2$G$_5$A$_2$G$_2$) to provide triple-stranded helices with mismatched base pairs. Continuous variation method established the formation of a 2:1 [d(Tg)$_4$-T-azido]$_2$·(pA$_n$pG$_m$) complex and also a 1:2 ratio between Ts and DNA bases.

In the denaturation/renaturation studies of the [d(Tg)$_4$-T-azido]$_2$·(pA$_n$pG$_m$) triplexes, all melting curves exhibit hysteresis. The dependence of T_{m} upon ionic strength has a slope of ca. −100 deg/(unit of ionic strength), a value twice as large as found in the interaction of d(Tg)$_4$-T-azido with short strand d(pA)$_x$ homooligomers. At 2.1×10^{-5} M/base concentration, the triplexes have well-defined T_{m} values only at $\mu < 0.12$ (*i.e.*, lower than the physiological ionic strength). At higher concentrations (*e.g.*, 6.3×10^{-5} M/base), one can differentiate between the four mismatched triplexes. In the physiological ionic strength range 0.15 − 0.30 and below, A$_5$G$_3$A$_5$ and GA$_4$G$_3$A$_4$G have well-defined T_{m} values which decrease with μ. The G$_2$A$_3$G$_3$A$_3$G$_2$ and G$_2$A$_2$G$_5$A$_2$G$_2$ oligomers do not have well-defined T_{m} values above $\mu = 0.12$! With the increase in the G content (mismatched base pairs) at a certain concentration (*e.g.*, 6.3×10^{-5} M/base), discrimination (change in fidelity) occurs in the formation and strength of binding of d(Tg)$_4$-T-azido to d(pA$_n$pG$_m$) oligomers.

At 15 °C, the second-order rate constants, k_{on}, for the triplex formation with A$_5$G$_3$A$_5$, GA$_4$G$_3$A$_4$G, G$_2$A$_3$G$_3$A$_3$G$_2$, and G$_2$A$_2$G$_5$A$_2$G$_2$ are between 10 and 500 M^{-1} s^{-1} (the molarity is expressed in per base) and the first-order rate constants k_{off} between 10^{-6} and 40×10^{-6} s^{-1} in the range $\mu = 0.06{-}0.24$. The values of k_{on} and k_{off} for A$_5$G$_3$A$_5$ are comparable with those for d(pA)$_{10}$. At G content of 23% in our A$_5$G$_3$A$_5$ 13-mer, the strength of the binding of d(Tg)$_4$-T-azido is not significantly changed [compared to d(pA)$_{10}$]. With the increase in the G content, both k_{on} and k_{off} change dramatically toward weaker binding. By decreasing the ionic strength, k_{on} increases, while k_{off} decreases. At G content lower than 23%, the triplexes behave similarly to short strand homooligomers [*e.g.*, d(pA)$_{10}$]. With the increase of the G content, the effect of the ionic strength on k_{on} and k_{off} is more marked, and in both cases there is a 4-fold change from A$_5$G$_3$A$_5$ (23% G) to G$_2$A$_2$G$_5$A$_2$G$_2$ (69% G).

At $\mu = 0.06$, the second-order rate constant with A$_5$G$_3$A$_5$ ($k_{\text{on}}^{15°\text{C}} \approx 400$ M^{-1} s^{-1}, molarity in per base) remains constant on increase in the concentration of reactants by a factor of 3, while maintaining the 2:1 ratio between d(Tg)$_4$-T-azido and DNA. The increase in $k_{\text{off}}^{15°\text{C}}$ on decrease in complex concentration ($6.3{-}2.1 \times 10^{-5}$ M/base) is much greater at higher G content of the DNA oligomers. This could be an indication that the dissociation process in the case of G-rich noncomplementary sequences is more complex and could involve intermediary steps.

With decrease in ionic strength, E_{on} decreases from −20 to −22 kcal/mol, whereas E_{off} increases from 10 to 14 kcal/mol. Also, the E_{on} values are negative and become generally less negative with the increase in the G content of the DNA oligomers, while the E_{off} values are positive and decrease with the increase in the G content of the DNA oligomers.

There is a better stabilization of the triplexes at low ionic strength and at low percent G of the DNA oligomers.

The variation in stability of short strand triple helices of G-rich DNA oligomers with d(Tg)$_4$-T-azido falls over a range of -8 to -12 kcal/mol with large negative values at low ionic strengths. The standard molar enthalpies $\Delta H°(288) = E_{\mathrm{on}} - E_{\mathrm{off}}$ are between -48.5 and -22.7 kcal/(mol base). A plot of $\Delta S°$ *vs* $\Delta H°$ shows a linear dependence and can be related to the enthalpy−entropy compensation for the $[\mathrm{d(Tg)_4\text{-}T\text{-}azido}]_2\cdot\mathrm{d(pA)}_x$ complexes.

ACKNOWLEDGMENT

This study was supported by the Office of Naval Research.

SUPPORTING INFORMATION AVAILABLE

Hypochromic shifts in the formation of $(\mathrm{d(Tg)_4\text{-}T\text{-}azido})_2\cdot\mathrm{d(pA_npG_m)}$ complex at 6.3 and 2.1×10^{-5} M/base and $\mu = 0.06-0.24$ at 10 °C. Ordering information is given on any current masthead page.

REFERENCES

Aboul-ela, F., Koh, D., Tinoco, I., Jr., & Martin, F. H. (1985) *Nucleic Acids Res. 13*, 4811−4824.

Albergo, D. P., Marky, L. A., Breslauer, K. J., & Turner, D. H. (1981) *Biochemistry 20*, 1409−1418.

Balagurumoorthy, P., & Brachmachari, S. K. (1994) *J. Biol. Chem. 269*, 21858−21869.

Blackburn, E. H., & Szostak, J. W. (1984) *Annu. Rev. Biochem. 53*, 163−194.

Blaskó, A., Dempcy, R. O., Minyat, E. E., & Bruice, T. C. (1996) *J. Am. Chem. Soc. 118*, 7892 −7899.

Breslauer, K. J. (1986) in *Thermodynamic Data for Biochemistry and Biotechnology* (Hinz, H.-J., Ed.) Chapter 15, Springer-Verlag, Berlin.

Breslauer, K. J., Sturtevant, J. M., & Tinoco, I., Jr. (1975) *J. Mol. Biol. 99*, 549−565.

Browne, K. A., Dempcy, R. O., & Bruice, T. C. (1995) *Proc. Natl. Acad. Sci. U.S.A. 92*, 7051−7055.

Cantor, C. R., & Schimmel, P. R. (1980) *Biophysical Chemistry*, Part III, W. H. Freeman and Co., San Francisco.

Cantor, C. R., & Tinoco, Jr., I. (1965) *J. Mol. Biol. 13*, 65−77.

Cantor, C. R., Warshaw, M. M., & Shapiro, H. (1970) *Biopolymers 9*, 1059−1077.

Chou, S-H., Zhu, L., & Reid, B. R. (1994) *J. Mol. Biol. 244*, 259−268.

Dempcy, R. O., Almarsson, Ö, & Bruice, T. C. (1994) *Proc. Natl. Acad. Sci. U.S.A. 91*, 7864−7868.

Dempcy, R. O., Browne, K. A., & Bruice, T. C. (1995a) *J. Am. Chem. Soc. 17*, 6140−6141.

Dempcy, R. O., Browne, K. A., & Bruice, T. C. (1995b) *Proc. Natl. Acad. Sci. U.S.A. 92*, 6097−6101.

Dempcy, R. O., Luo, J., & Bruice, T. C. (1996) *Proc. Natl. Acad. Sci. U.S.A. 93*, 4326−4330.

Ebel, S., Lane, A. N., & Brown, T. (1992) *Biochemistry 31*, 12083−12086.

Evans, T., Schon, E., Gora-Maslak, G., Patterson, J., & Efstratiadis, A. (1984) *Nucleic Acids Res. 12*, 8043−8058.

Gray, D. M., Hung, S.-H., & Johnson, K. H. (1995) in *Methods in Enzymology*, Vol. 246, p 19, Academic Press, New York.

Guckian, K. M., Scheweitzer, B. A., Ren, R. X.-F., Sheils, C. J., Paris, P. L., Tahmassebi, D. C., & Kool, E. T. (1996) *J. Am. Chem. Soc. 118*, 8182−8183.

Hirao, I., Kawai, G., Yoshizawa, S., Nishumura, Y., Ishido, Y., Watanabe, K., & Miura, K.-i. (1994) *Nucleic Acids Res. 22*, 576−582.

Howard, F. B., Miles, H. T., & Ross, P. D. (1995) *Biochemistry 34*, 7135−7144.

Hüsler, P. L., & Klump, H. H. (1994) *Arch. Biochem. Biophys. 313*, 29−38.

Jaskunas, S. R., Cantor, C. R., & Tinoco, I., Jr. (1969) *Biochemistry 7*, 3164−3178.

Jin, R., Gaffney, B. L., Wang, C., Jones, R. A., & Breslauer, K. J. (1992) *Proc. Natl. Acad. U.S.A. 89*, 8832−8836.

Ke, S.-H., & Wartell, R. M. (1996) *Nucleic Acids Res. 24*, 707−712.

Kilpatrick, M. W., Torri, A., Kang, D. S., Engler, J. A., Wells, R. D. (1986) *J. Biol. Chem. 261*, 11350−11354.

Kochoyan, M., & Leroy, J. L. (1995) *Curr. Opin. Struct. Biol. 5*, 329−333

Maher, L. J., Dervan, P. B., & Wold, B. J. (1990) *Biochemistry 29*, 8820−8826.

Marky, L. A., & Breslauer, K. J. (1987) *Biopolymers 26*, 1601−1620.

Mergny, J.-L., Lacroix, L., Han, X., Leroy, J.-L., & Hélène, C. (1995) *J. Am. Chem. Soc. 117*, 8887−8898.

Mitchell, J. E., Newbury, S. F., & McClellan, J. (1995) *Nucleic Acids Res. 23*, 1876−1881.

Modrich, P. (1987) *Annu. Rev. Biochem. 56*, 435−466.

Olivas, W. M., & Maher, J., III (1995) *Biochemistry 34*, 278−284.

Patten, J. E., So, A. G., & Downey, K. M. (1984) *Biochemistry 23*, 1613−1618.

Petersheim, M., & Turner, D. H. (1983) *Biochemistry 22*, 256−263.

Petruska, J., & Goodman, M. F. (1995) *J. Biol. Chem. 270*, 746−750.

Pilch, D. S., Plum, G. E., & Breslauer, K. J. (1995) *Curr. Opin. Struct. Biol. 5*, 334−342.

Plum, G. E., & Breslauer, K. J. (1995) *J. Mol. Biol. 248*, 679−695.

Rougée, M., Faucon, B., Mergny, J. L., Barcelo, F., Giovannangeli, C., Garestier, T., & Hélène, C. (1992) *Biochemistry 31*, 9269−9278.

Rouhi, M. (1996) *CChem. Eng. News* Sept 9, 38−39.

Sanghvi, Y. S., & Cook, P. D. (1993) in *Nucleosides and Nucleotides and Antiviral Agents* (Chu, C. K., & Baker, D. C., Eds.) p 331, Plenum Press, New York.

Sen, D., & Gilbert, W. (1990) *Nature 334*, 410−414.

Shimizu, A., & Honjo, T. (1984) *Cell 36*, 801−803.

Su, S.-S., Lahue, R. S., Au, K. G., & Modrich, P. (1988) *J. Biol. Chem. 263*, 6829−6835.

Uhlenbeck, O., & Harrison, R. (1968) in *Molecular Associations in Biology* (Pullman, B., Ed.) p 107−114, Academic Press, New York.

Van Meervelt, L., Vlieghe, D., Dautant, A., Gallois, B., Précigoux, G., & Kennard, O. (1995) *Nature 374*, 742−744.

Vasseur, J.-J., Debart, F., Sanghvi, Y. S., & Cook, P. D. (1992) *J. Am. Chem. Soc. 114*, 4006−4007.

Vesnaver, G., & Breslauer, K. J. (1991) *Proc. Natl. Acad. Sci. U.S.A. 88*, 3569−3573.

Vo, T., Wang, S., & Kool, E, T. (1995) *Nucleic Acids Res. 23*, 2937−2944.

Watson, J. D., & Crick, F. H. C. (1953) *Nature 171*, 964−967.

Wilson, W. D., Hopkins, H. P., Mizan, S., Hamilton, D. D., & Zon, G. (1994) *J. Am. Chem. Soc. 116*, 3607−3608.

BI970064V